THE EUROPEAN SOCIETY OF MEDICINE
Medical Research Archives, Volume 12 Issue 8

RESEARCH ARTICLE

An Accurate Algebraic Closed Form Solution for Drug Transport Kinetics through P-Glycoprotein Expressing Confluent Cell Monolayers by Fitting Our Experimentally Derived Empirical Fitting Function with the Elementary Rate Constants of 370 Virtual P-gp substrates

Joe Bentz[1] & Harma Ellens[2]

[1]Drexel University, Philadelphia, PA.
[2]GlaxoSmithKline, King of Prussia, PA.

OPEN ACCESS

PUBLISHED
31 August 2024

CITATION
Bentz, J., & Ellens, H., 2024. An Accurate Algebraic Closed Form Solution for Drug Transport Kinetics through P-Glycoprotein Expressing Confluent Cell Monolayers by Fitting Our Experimentally Derived Empirical Fitting Function with the Elementary Rate Constants of 370 Virtual P-gp substrates. Medical Research Archives, [online] 12(8). https://doi.org/10.18103/mra.v12i8.5738

DOI
https://doi.org/10.18103/mra.v12i8.5738

ISSN
2375-1924

ABSTRACT

The kinetics of transport by P-gp through confluent cell monolayers is typically modelled by a version of the Michaelis-Menten equations within PBPK mechanistic models[1-5]. The quasi-steady-state Michaelis-Menten equation was solved by the Lambert W-function, which is an infinite summation series that can only be evaluated in Matlab, Maple and a few other math programs[6]. Our Structural Mass Action Kinetic Model (SMAKM) for P-gp transport through confluent cell monolayers was built from a more accurate set of mass action kinetic equations. Its most significant departure from PBPK mechanistic models was that P-gp can only bind drug that has partitioned from the cytosol into the cytosolic monolayer, according to its molar partition coefficient $K_{PC,}$ since that is where P-gp's substrate binding site resides. Our analysis of P-gp transport for many drugs using SMAKM has shown that most, if not all, commonly used P-gp expressing cells also express basolateral and apical uptake transporters for many, if not all, P-gp substrates. An algebraic Closed Form Solution for P-gp transport has been built by fitting the elementary rate constants of 370 Virtual P-gp substrates to an algebraic equation we started building in 2005 to fit our experimental drug transport kinetics through P-gp expressing confluent cell monolayers. The resultant algebraic Closed Form Solution clearly shows how each of P-gp's elementary rate constants contributes to transport. It is currently used, within Excel, to predict the upper and lower bounds required to fit the elementary rate constants of new experimental drug transport data using Matlab's Particle Swarm program.

The clearest evidence that SMAKM was an accurate mass action description for P-gp transport through confluent cell monolayers was our discovery that substrates with passive permeabilities less than 400 nm/s could not be well-fitted with only P-gp[7-10]. These data kinetically required the presence of uptake transporters for P-gp substrates in both the basolateral and apical membranes. These uptake transporters have never been reported in the literature of the PBPK mechanistic model. The contribution of uptake transporters was likely absorbed into other kinetic parameters. We have shown that Uptake transporters are kinetically insignificant for drugs with passive permeabilities exceeding about 400 nm/s[10].

All of our experimental drug kinetic rate constants were fitted using numerical integration of SMAKM's mass action differential equations, using a Particle Swarm program developed at Glaxo SmithKline[8]. The fitting process was lengthy, but eventually yielded straightforward and unambiguous results for the 7 drugs we analyzed over the years[7,10,11]. That Particle Swarm program is no longer available, however Mathworks has a Particle Swarm directed numerical integration routine which we are currently using.

Here we show how an approximate closed-form solution for SMAKM's mass action differential equations was derived that is accurate within experimental error with the confluent cell monolayers used to study P-gp efflux. It is highly unlikely that SMAKM's ODE will be mathematically integrated into an exact solution, as was recently accomplished for the steady-state Michaelis-Menten reaction at the core of the PBPK mechanistic models for P-gp transport kinetics[6]. The exact solution is a Lambert W-function, which is an infinite series summation of a function that currently must be evaluated online using MathWorks or other similar sites. This solution is exact for this kinetic model, but not very clarifying mechanistically.

Our first paper on drug transport through confluent cell monolayers was focused on accurately fitting the passive permeability[12]. It introduced our novel data acquisition protocol, which assumed that the amphipathic P-gp substrates injected into the Transwell apparatus would initially partition into all available "amphipathic sites", including those within the Transwell plate[13].

To allow this partitioning to pre-equilibrate before measuring real transport, the initial experimental data concentration for the donor $C_D(t_0)$ and receiver $C_R(t_0)$ was taken at t_0=0.25h after drug addition. Subsequent donor $C_D(t)$ and receiver $C_R(t)$ data concentrations were obtained for t=0.5, 1, 2, 3, 4, 5 & 6hr. This data acquisition protocol was used for all our experiments, with a single exception[7] discussed below.

Our second paper introduced the Structural Mass Action Kinetic Model (SMAKM)[11]. P-gp efflux was rigorously defined by elementary rate constants.

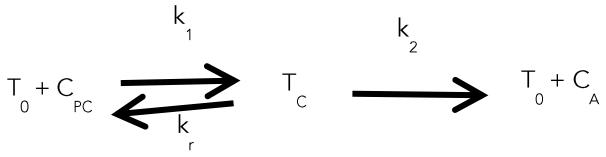

(1)

T_0 (empty P-gp), T_C (drug bound P-gp), C_{PC} (drug partitioned from cytosol into inner cytosolic monolayer by its molar partition coefficient, K_{PC}), C_A (drug effluxed by P-gp into apical chamber), and $T(0) = [T_0] + [T_C]$ is the total efflux active P-gp, i.e. those P-gp whose efflux reaches the apical aqueous chamber, as opposed to being reabsorbed into neighboring microvilli.

Unexpectedly, fitting the amprenavir, loperamide and quinidine data showed that only a small fraction of the P-gp in the apical membrane effluxed drug into the apical aqueous chamber[11]. Our hypothesis was only the P-gp expressed at the tips of the microvilli was "efflux active", while efflux from P-gp residing below the microvilli tips would collide into adjacent microvilli membranes and partition back into that membrane in a futile cycle[11]. Cell biology later supported this hypothesis. During cell fertilization, actin polymerization moves P-gp to microvillus tips, which significantly increases total cell efflux[14].

Meng et al.[15,16] quantitatively validated this hypothesis by showing that only 11% of P-gp in Caco-2 cells was efflux active, while 63% of P-gp in MDCKII-hMDR1-NKI cells was efflux active. To understand this difference, Ellens et al.[17] used 3D SIM microscopy to show that the microvilli "forest" of Caco-2 cells was upright and closely packed together, while the MDCKII microvilli "forest" had neither of those features. Clearly, total cell P-gp is irrelevant to accurately fitting P-gp transport kinetic rate constants for confluent cell monolayers.

SMAKM's elucidation of the existence of other drug transporters in P-gp expressing cells was first shown in Acharya et al[7]. Our P-gp expressing cells kinetically required a Basolateral Uptake Transporter clearance value of k_B=40 s^{-1} for digoxin transport within 6 hrs. In order to confirm the existence of an Apical Uptake Transporter clearance value of k_A=40 s^{-1} for digoxin transport in these cells, it was necessary to obtain data over 30 hrs, using sequential 6h experiments[7]. Lumen et al.[10] showed that while the passive permeabilities of verapamil and ketoconazole were too large, >400 nm/s, to allow direct kinetic evidence that they were transported by Uptake Transporters, both drugs specifically inhibited digoxin transport through the Basolateral Uptake Transporter in MDCK-MDR1-NIH, Caco-2 and CPT-B2 cells. Chaudhry et al.[18] showed that Basolateral Uptake Transporters for digoxin were kinetically required in human primary proximal tubule cells, HPTC, as well as in the Caco-2, LLC-PK and MDCK cells of the 5 labs with most rigorous data from the 2013 IC_{50} Initiative of 24 pharmaceutical companies[19-21]. Table 1 below shows our fitted values for these Uptake Transporter clearances, denoted k_B and k_A. These Uptake Transporters has not been otherwise reported in the literature.

Early on in our fitting of P-gp substrates, it was clear that the simplest equation that fitted our data for drug concentration in the receiver chamber over time, $C_R(t)$, was simply exponential:

$$C_R(t) \approx C_R(t_{SS})*[1-A*\exp\{-k*(t-t_0)\}] \quad (2)$$

$C_R(t_{SS})$ was the steady-state of the experiment, estimated after 6 or more hours, A was the fitted amplitude and k was the fitted rate constant. The next step was figuring out which elementary kinetic rate constants in SMAKM defined the values of $C_R(t_{SS})$, A and k. This required transport kinetic data for many more substrates than were experimentally feasible.

The first usage of Virtual Drugs was to discover whether SMAKM had a first order rate constant for efflux active P-gp, resembling the Michaelis-Menten steady-state V_{max}/K_M. This was accomplished, but unpublished, in 2021 by creating 200 Virtual P-gp substrates. The first order rate constant was defined $H_0 \equiv k_1 k_2 T(0)/k_r$. For H_0 values ranging from 2.5 to 31, k_r and k_2 values of digoxin were varied 3-fold, which included all of our experimental drugs. T(0) was varied 3-fold for cell line dependency in the range of (0.2-1)e-3 M, based on the cell lines we had analyzed. k_1=1e8 $M^{-1}s^{-1}$ remained fixed for all drugs (Tran et al., 2005). For each H_0 value, all combinations of T(0), k_2 and k_r yielded the same SMAKM numerically integrated transport concentrations up to 6 hours, $C_R(t)$, within ±9%. Clearly, H_0 was SMAKM's first order rate constant, which resembles Vmax/Km, but without the steady-state assumptions.

The analysis of these results transformed our Empirical Fitting Equation to its current version, with its experimentally measured and fitted Essential Kinetic Functions (EKF) in bold.

$$C_R(t) \simeq \boldsymbol{C_R(t_{SS})}\left[1-\left(1-\frac{\boldsymbol{C_R(t_0)}}{\boldsymbol{C_R(t_{SS})}}\right)exp\{-(H_0+1)k_{PP}\boldsymbol{f_H}*(t-t_0)\}\right] \quad (3)$$

$C_R(t)$: Receiver drug concentration at time t, with values at t(h)=0.1, 0.25, 0.5, 1, 2, 4, 6 hours for experiments, while simulations included 8, 12 & 100 hours.

$C_R(t_0)$: Initial concentration of drug in the receiver chamber at t_0=0.25h after drug addition to the donor chamber for pre-equilibration.

$C_R(t_{SS})$: Final steady-state concentration in the receiver chamber, estimated at 6h for experiments and defined at 100h for simulations.

$C_R(t_1)$: Concentration of drug in the receiver chamber at t_1=0.5h, which is the first experimental data point due solely to the kinetics of transport. Its fitted algebraic function was required to build the algebraic functions of $C_R(t_0)$ and $C_R(t_{SS})$ for the Closed Form Solution, as shown in the Supplemental Material.

f_H: The best fit parameter for data or simulations, which quantitates the kinetic correlations between passive permeability, P-gp efflux and Uptake Transporters, for each experimental and Virtual drug. It is independent of transport direction and initial drug concentrations in the range of 0.01-10μM for 12-well Transwell data.

H_0: 1st order rate constant for P-gp efflux, defined above. H_0+1 is used in the equation to accommodate P-gp inhibition studies, where H_0=0

k_{PP} = 4.52e-7*[P_{AB}*P_{BA}/(P_{AB}+P_{BA})]s^{-1} is the average passive permeability rate constant across the confluent cell monolayer[12]. It is the sole transport rate constant with added Elacradir (previously known as GF120918), which completely inhibits P-gp and Uptake Transporters, i.e. H_0=0 and f_H=1, with passive permeability measured as P_{AB} in the A>B direction and P_{BA} in the B>A direction, which are typically different, Table 1.

U_{PP}: Unified passive permeation rate constants which are in the mass action kinetic ordinary differential equations for SMAKM, as shown in Supplemental Material.

U_A=2.26x10^{-7}*[P_{AB}(nm/s) + 2.5*$k_A(s^{-1})$] cm^3/s
U_B=2.26x10^{-7}*[P_{BA}(nm/s) + 2.5*$k_B(s^{-1})$] cm^3/s
U_H= U_A*U_B/(U_A+U_B)

Eq. (3) is the template for our Closed Form Solution for P-gp transport kinetics through confluent cell monolayers. Numerical integration by SMAKM's ODE of the rate constants of a Virtual P-gp substrate yields exact values for $C_R(t_0)$, $C_R(t_1)$, $C_R(t_{SS})$ and $C_R(t)$. Building the algebraic functions of the kinetic parameters that define the value of each EKF transforms the Empirical Fitting Function into a Closed Form Solution for the kinetics of P-gp mediated transport through confluent cell monolayers. We used the kinetic rate constants (KP) of 370 Virtual Drugs to fit these algebraic functions, as described in the Supplemental Material of this paper. The values of our experimentally fitted kinetic parameters in Table 1 were used to construct useful ranges for these Virtual Drugs, as described in the Supplemental Material.

Table 1: Elementary Rate Constants for experimentally fitted drugs in several P-gp expressing cell lines

Drug	Cells	k_2 (s^{-1})	k_r (s^{-1})	H_0 (s^{-1})	P_{AB} (nm/s)	P_{BA} (nm/s)	k_A (s^{-1})	k_B (s^{-1})	K_{PC}
Amprenavir	MDCK Caco	30 10	7e4 6e4	15	420	440	?	?	100
Digoxin	MDCK Caco, LLC-PK HPTC	3 9	3e4 2e4	10 45	40	50	40	40 30 5 2-45	100
Ketoconazole	MDCK	0.2	3e4	0.7	730	680	?	**?!**	1000
Loperimide	MDCK Caco	0.4 0.3	2e4 6e4	1	190	130	?	100 20	1500
Quinidine	MDCK Caco	3 1	4e3 1e4	25	670	670	?	?	350
Vinblastine	MDCK	3	5e4	6	55	90	?	60	200
Verapamil	MDCK	0.1	2e4	0.5	540	580	?	**?!**	650

For all cell lines and experimental drugs: T(0)=(0.2-1)e^{-3} M and k_1=1e8 $M^{-1}s^{-1}$

The? for the Uptake Transporter clearances k_A and k_B means that it could not be fitted because the drug's passive permeability was >400 nm/s or, in the case of loperamide and vinblastine, the A>B experimental data was inadequate. The**?!** means that the Ketoconazole and Verapamil k_B is kinetically insignificant, but that both drugs specifically inhibit digoxin transport through the Basolateral Uptake transporter. The experimentally measured values of P_{AB} and P_{BA} with Elacradir vary somewhat with drug concentration, presumably due to microvilli morphology changes, e.g. as with efflux active P-gp. The asymmetries between P_{AB} and P_{BA} are likely due to the same mechanism. Basically, confluent cell monolayers respond to their drug environment.

Each Virtual Drug (VD) was defined by unique vector of values:

$$KP_{VD}=(k_1, T(0), k_2, k_r, k_A, k_B, P_{AB}, P_{BA}, K_{PC}) \quad (4)$$

Each KP_{VD} described below was numerically integrated by SMAKM's ODE, Eq. (9) in the Supplemental Material, for t(h)=0.1, 0.25, 0.5, 1, 2 , 4, 6, 8, 12 & 100 hours, for the initial drug concentrations $C_D(0)$=0.001, 0.01, 0.1, 1 & 10 μM, for both A>B and B>A transport. This yields the simulation values for the transport concentration time course, $C_R(t)$, as well as the values of the Essential Kinetic Functions [$C_R(t_0$=0.25h), $C_R(t_1$=0.5h), $C_R(t_{SS}$=100h)] for the range of drug concentrations that are found or used in vitro and in vivo.

KP_{VD} vectors were created for three families of Virtual Drugs to produce a broad enough data set to be able to yield a Closed Form Solution that was accurate within experimental error:

1) The Medial family had 126 KP_{VD} vectors roughly centered on digoxin, our most completely fitted P-gp substrate. The fitting focus was discovering the basic relationships between the Essential Kinetic Functions and the unified passive permeation rate constants, U_A and U_B. Digoxin's value of K_{PC}=300 was used for this family.

2) The Primal family had 40 KP_{VD} vectors centered on how P-gp transport kinetics were altered by the "emergence" of Uptake transporters in P-gp expressing cells. K_{PC}=300 was also used for this small family.

3) The Cytosolic Monolayer Control family had 205 KP_{VD} vectors centered on discovering the effect of K_{PC} on drugs that have very asymmetric U_A and U_B values, e.g cells expressing only one Uptake transporter. K_{PC} was 100, 300 or 1000, which covered most of the experimentally known drug range.

In order to facilitate access to this analysis of P-gp transport kinetics, only algebraic functions in Excel were used to build the equations that fitted these EKF within an Excel spreadsheet. For the Medial and Primal families these fitted equations are derived in Eqs. (10-13) in the Supplemental Material. The CMC family required an additional fitting step for the $C_R(t_1)$fit function, as shown in the Supplemental Material, which varied one of the coefficients in these equations. This is shown in detail in the Supplemental Material and is in our Excel spreadsheet that makes these calculations for each Virtual Drug and experimental data, which is available on request. However, the description is somewhat complex, so the EKF functions shown here apply to the Medial and Primal families.

The equations for each fitted EKF is denoted by "fit" on the its name:

$$C_R(t_1,A>B)_{fit}=3.4e5*U_H\text{^}[1.75*[(H_0+1)\text{^}\{0.031\}]]/[[4.7e3*K_{PC}\text{^}0.94]*[(H_0+1)\text{^}\{0.47\}]]$$

$$C_R(t_1,B>A)_{fit}=[24*(H_0+1)\text{^}\{0.52\}]*[U_B\text{^}\{0.83*(H_0+1)\text{^}\{0.048\}\}] \quad (5)$$

$$C_R(t_0,A>B)_{fit}=0.44*[C_R(t_1,A>B)fit\text{^}\{0.98\}] \quad (6)$$

$$C_R(t_0,B>A)_{fit}=0.46*[C_R(t_1,B>A)fit\text{^}\{0.98\}]$$

$$C_R(t_{SS},A>B)_{fit}=0.44*[1.6x10^3/[U_B\text{^}\{0.96\}]]*[C_R(t_1,A>B)_{fit}\text{^}\{0.98\}] \quad (7)$$

$$C_R(t_{SS},\ B>A)_{fit}=\ 0.46*[1.6x10^{-3}/[U_B\text{^}\{0.96\}]]*[C_R(t_1,B>A)_{fit}\text{^}\{0.98\}]$$

$$f_Hfit=[0.10+1.9*U_B/(P_{AC}+P_{BC})]/(H_0+1), \text{ in both directions} \quad (8)$$

$C_R(t_1,A>B)$ depends on value of K_{PC}, which defines the values of $C_R(t_0$, A>B) and $C_R(t_{SS}$, A>B). B>A transport did not significantly depend on K_{PC}. The

value of $f_H$fit does not depend on K_{PC}, k_A or transport direction.

The final accuracy of C_R(t)fit relative to the exact simulation values of C_R(t)sim for all 3 families, i.e. including the final CMC family values, for C_D(0)=0.1 μM was quantified by:

<Rerr(t)>= the average of [C_R(t)fit/C_R(t)sim -1]% over all times t(h)=0.5-100h
<ABS(Rerr(t))>= average of absolute value of the relative error over all times t(h)=0.5-100h

The closed form solution fitted well within experimental error:

A>B 40 PRM fits: <Rerr(t)> = -1% and <ABS(Rerr(t))> = 2%
126 MDL fits: <Rerr(t)> = -3% and <ABS(Rerr(t))> = 4%
204 CMC fits: <Rerr(t)> = 1% and <ABS(Rerr(t))> = 6%
B>A 40 PRM fits: <Rerr(t)> = -2% and <ABS(Rerr(t))> = 3%
126 MDL fits: <Rerr(t)> = -1% and <ABS(Rerr(t))> = 3%
204 CMC fits: <Rerr(t)> = 3% and <ABS(Rerr(t))> = 4%

The closed form solution was not biased toward under- or over-estimates and was sufficiently accurate to be used with experimental data to fit transporter kinetics. For C_D(0) up to1.0 μM, the fits for C_R(t) were within 5% of the simulated values up to 12 hrs in both directions. The fits for C_D(0)=10μM was slightly worse, but within experimental error. Details of this fitting are described in the Supplemental Materials, as well as the additional steps required to fit the CMC family that yielded these <Rerr(t)> and <ABS(Rerr(t))> percentages.

This closed form solution also fitted our 7 drugs[10], i.e. amprenavir, loperamide, quinidine, digoxin, verapamil, vinblastine and ketoconazole, well within experimental error. Using the closed form solution is not as accurate as using Particle Swarm, but we have used it to optimize the experimental fitting of kinetic parameters for many drugs. Most importantly, it clearly shows how all the KP interact to create transport kinetics.

The Structural Mass Action Kinetic Model (SMAKM) differs significantly from the standard PBPK mechanistic model:

1) SMAKM has no steady-state assumptions.

2) Only "Efflux active" P-gp near microvilli tips yields significant transport. Total cell P-gp is essentially irrelevant to fitting transport kinetic parameters.

3) SMAKM kinetically required basolateral and apical uptake transporters (UT) for digoxin and loperamide in MDCKII-hMDR1-NKI and, at least for digoxin, in the basolateral membrane of primary Human Proximal Tubule Cells, Caco2 and LLC-PK cells. These transporters are not in PBPK mechanistic models

4) Remarkably, while the passive permeabilities of verapamil and ketoconazole are too large to allow direct fitting evidence of their UT transport, both drugs specifically inhibited digoxin transport through the basolateral Uptake Transporter in Caco-2 and MDCKII cells[10].

P-gp binds drug that has reached the cytosolic monolayer according to its molar partition coefficient K_{PC} with the cytosol of the cell. Currently, K_{PC} is estimated by binding to liposomes composed of lipids that mimic the cell's cytosolic monolayer. This K_{PC} for our drugs poorly correlates with their literature value for Octanol/H_2O logP values used by the standard PBPK mechanistic models, as shown in Fig. 1 below.

Fig. 1 shows that the literature values of Octanol/Water K_{OW} values correlate poorly on a log-log plot with the molar partition K_{PC} for our 7 P-gp substrate drugs.

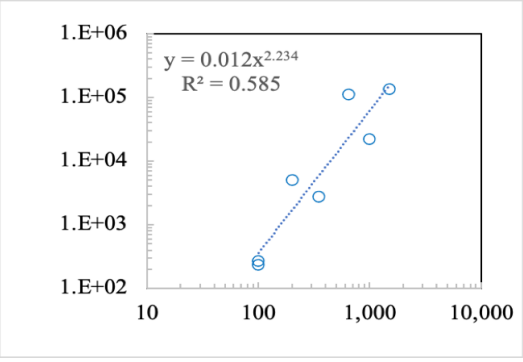

This closed form solution for P-gp transport kinetics, can be easily adapted to fit the transport kinetics for other "Typical" or "Atypical" membrane transporters

Supplemental Material

The Structural Mass Action Kinetic Model equations for P-gp transport through confluent cell monolayers, without drug inhibitors, are shown in Eq. 1, Lumen et al.[10]. C_A, C_B and C_C denote the substrate concentrations in the apical, basolateral and cytosol aqueous compartments

$$\bar{V}_B \frac{dC_B}{dt} = -U_B(C_B - C_C)$$
$$\bar{V}_A \frac{dC_A}{dt} = -U_A(C_A - C_C) + V_{AO}k_2T_C$$
$$\bar{V}_C \frac{dC_C}{dt} = U_A(C_A - C_C) + U_B(C_B - C_C) + V_{AO}k_rT_C - V_{AO}k_1K_{PC}C_CT_0 \quad (9)$$
$$\frac{dT_C}{dt} = k_1K_{PC}C_CT_0 - (k_r + k_2)T_C$$

$k_1(M^{-1}s^{-1})$ is the rate constant for substrate binding to P-gp within inner plasma membrane. $k_2(s^{-1})$ is the rate constant for substrate efflux from P-gp to the apical chamber. $k_r(s^{-1})$ is the rate constant for substrate dissociation from P-gp back into the inner plasma membrane. The unified passive portals U_A and U_B are defined in main paper. $V_{AO} = V_{BO} = 5.65x10^{-7}cm^3$ are the estimated lipid volume of the outer apical and basolateral monolayers of the plasma membrane, which determines the efflux active P-gp concentration in the apical membrane. T_0 is the membrane concentration of empty efflux active P-gp and T_C is the membrane concentration of efflux active P-gp with its single binding site bound by drug (14). The total concentration of efflux active P-gp is denoted $T(0)=T_C+T_0$.

These required volumes were shown in Lumen et al.[10], and are:

V_A = volume of Transwell apical chamber (0.5 mL)

$\bar{V}_A = V_A + K_{AO}V_{AC}$ Entire apical volume accessible to substrate,

V_B = volume of Transwell basolateral chamber (1.5 mL)

$\bar{V}_B = V_B + K_{BO}V_{BO}$ Entire basolateral volume accessible to substrate,

V_C = volume of entire cell monolayer cytosol (roughly 1µL)

$\bar{V}_C = V_C + K_{PC}V_{PC}$ Entire cytosolic volume accessible to substrate,

K_{AO} and K_{BO} are the molar partition coefficients of the substrate to the apical and basolateral outer cell monolayers, like K_{PC}, as estimated by drug binding to liposomes in Lumen et al[10]. All of these terms and values are defined in the Supplemental Material of Lumen et al[10]. They are also in our Excel spreadsheet that makes these calculations for each Virtual Drug and experimental data, which is available on request.

Using SMAKM's ODE to simulate concentration data over time was the next step to create an accurate closed form approximate solution for our mass action kinetic model. To have sufficient data to accomplish this task, the 3 families of virtual drugs described in the paper were created. Each family was populated by vectors of Virtual Drug rate constants, denoted as $KP_{VD}=(k_1, T(0), k_2, k_r, k_A, k_B, P_{AB}, P_{BA}, K_{PC})$. The values of the elementary rate constants for T(0), k_2 and k_r were chosen to define the H_0 values required in that family. The numerical integration of Eq. (9) for each KP_{VD} vector yielded the concentrations of the **Essential Kinetic** Functions, i.e. $C_R(t_0)$, $C_R(t_1)$, $C_R(t_{SS})$ and $C_R(t)$, for that vector's rate constants. Each could depend on one or more rate constants, while all were well fitted by simple algebraic equations within the Excel spreadsheet, as shown below. The diffusion limited value of $k_1=1e^8$ $M^{-1}s^{-1}$ was assumed constant over all drugs and cell lines, until proven otherwise[10].

Our 3 families of Virtual Drugs were chosen to populate the KP_{VD} space defined by our 7 drugs in Table 1 of the main paper and to include likely newcomers. However, passive permeabilities greater than 450 nm/s were omitted, since Lumen et al.[10] showed that uptake transporters are kinetically insignificant when passive permeabilities exceed 400 nm/s. Half of our 7 drugs had these larger passive permeabilities, yet they were well fitted by our Closed Form Solution.

For the Medial Family (126 KP_{VD}):

T(0)=1e-3 M for MDCKII cells, Lumen et al.[10]

k_2 ranged from 0.4-3.0 s^{-1} and k_r ranged from 2e4 - 5e4 s^{-1}.

Values for k_2 and k_r were chosen to yield $H_0(s^{-1})$ = (2, 6, 10, 15)

For the Primal Family (40 KP_{VD}):

T(0)=3e-4 M for Caco-2 cells, Meng et al.[15,16]

k_2 ranged from 2-4.5 s^{-1} and k_r ranged from 1.5e4 - 4e4 s^{-1}.

Values for k_2 and k_r were chosen to yield $H_0(s^{-1})$ = (1.5, 3, 9)

For the Cytosolic Monolayer Control Family (204 KP_{VD}):

T(0)=1-2e-3 M for both MDCKII cell lines, Chaudhry et al.[18]

k_2 ranged from 2.0-3.0 s^{-1} and k_r ranged from 2e4 - 4e4 s^{-1}

Values for k_2 and k_r were chosen to yield $H_0(s^{-1})$ = (5, 10, 15, 30)

The remaining passive permeabilities, Uptake transporter clearances and cytosolic molar partition coefficients for the 370 Virtual Drugs were chosen as follows.

The Medial family with 126 simulations was roughly centered on the experimentally measured KP for digoxin, loperamide and vinblastine.

H_0 s^{-1}	P_{AC} nm/s	P_{BC} nm/s	k_A s^{-1}	k_B s^{-1}	K_{PC}
2, 6, 10, 15	40, 100, 150, 450	50, 100, 150, 450	0, 1, 3, 15, 40	ditto	300

The Primal family with 40 simulations had a focus on how to best determine whether the cells kinetically required uptake transporters.

H_0 s^{-1}	P_{AC} nm/s	P_{BC} nm/s	k_A s^{-1}	k_B s^{-1}	K_{PC}
1.5, 3, 9	50, 100, 250, 300, 350	ditto	0, 1, 2, 5	ditto	300

The CMC family with 204 simulations had a sparse, but broad, KP range, with a focus on the effect of K_{PC} and highly asymmetric Uptake Transporter clearances on fitting transport kinetics.

H_0 s^{-1}	P_{AC} nm/s	P_{BC} nm/s	k_A s^{-1}	k_B s^{-1}	K_{PC}
5, 10, 15, 30	30, 60, 200	ditto	0, 10, 60	ditto	100, 300, 1000

While the Medial and Primal families were unified by a single K_{PC} value, the CMC family had 3 "clans" because of their 3 K_{PC} values. Furthermore, a schism showed up in the K_{PC}=100 Clan, which segregated those with P_{AB} and P_{BA} values were equal from those with different values, yielding 2 subclans of KP_{VD}. This will be clarified in the Amelioration Table description below

The SMAKM numerical integrations of each KP_{VD} yielded the values of the essential functions, i.e. $C_R(t_0)$, $C_R(t_1)$ and $C_R(t_{SS})$, as well as $C_R(t)$. Fitting these essential function data, using Excel's chart fitting functions to keep it simple and accessible, has yielded simple accurate algebraic equations for all, that clearly show how each kinetic parameter contributes to drug transport.

The first essential function to be fitted was $C_R(t_1)$, since it turned out to be required to obtain the functional forms of $C_R(t_0)$ and $C_R(t_{SS})$. Fig. (2) shows the simulation values of $C_R(t_1)$ for the Medial Family, which depended only on the Unified Passive Permeation constants. Clearly, the Essential Kinetic Function $C_R(t_1)$ strongly depended on transport direction.

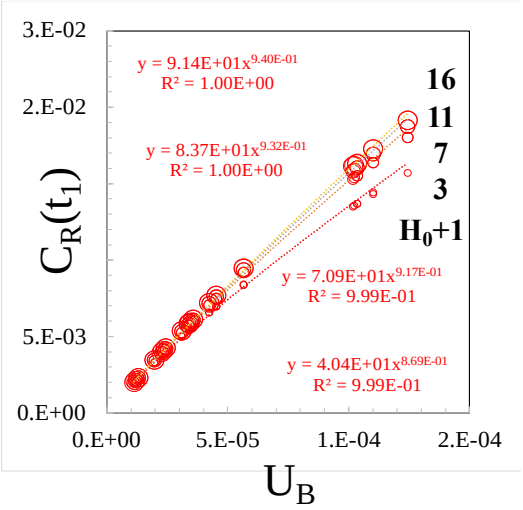

Fig 2A is the plot of $C_R(t_1,B>A)$ as a function of U_B

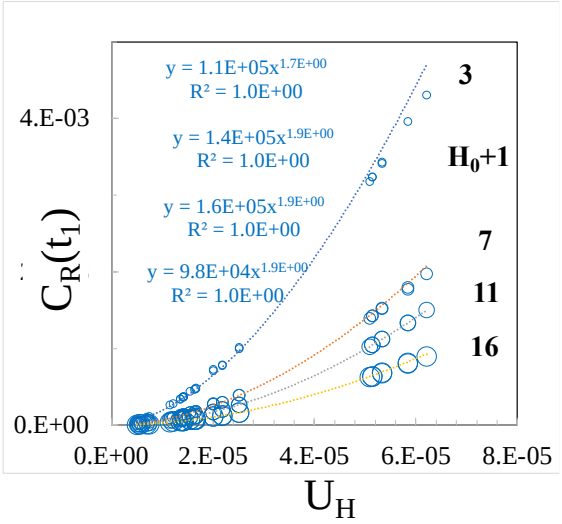

Fig 2B is the plot of $C_R(t_1,A>B)$ as a function of $U_H=U_AU_B/(U_A+U_B)$

$U_H=(U_A*U_B)/(U_A+U_B)$ is simply the net passive permeation constant across two barriers, just like the net passive permeability of P_{AB} and P_{BA}[12]. A>B transport will be analyzed first, simply because it was experimentally more complex and would yield more detailed information. For example, B>A transport, does not significantly depend on H_0 for U_B<1e-4 cm^3/s. After the A>B function for $C(t_1)$ was fitted, deriving the B>A function for $C_R(t_1)$ was relatively straightforward.

For the Medial and Primal families,
$C_R(t_1,A>B)fit=Bn/Bd$, where
$Bn=b(1)*U_H\text{^}\{b(3)*(H_0+1)\text{^}\{b(4)\}\}$
$Bd=[b(5)*K_{PC}\text{^}b(6)]*[(H_0+1)\text{^}\{b(2)\}]$ (10a)

40 PRM fits: <Rerr> = -4% <ABS(Rerr)> = 4%
126 MDL fits: <Rerr> = -3% <ABS(Rerr)> = 5%

$C_R(t_1,B>A)fit=[b(1)*(H_0+1)\text{^}b(2)]*[U_B\text{^}\{b(3*(H_0+1)\text{^}b(4)\}]$. (10b)

40 PRM fits: <Rerr> = -1% <ABS(Rerr)> = 2%
126 MDL fits: <Rerr> = 0% <ABS(Rerr)> = 2%

The b-coefficients that best fitted Eqs. 10a & 10b were:

	b(1)	b(2)	b(3)	b(4)	b(5)	b(6)
A>B	3.41e5	0.470	1.75	3.10e-2	4.70e3	0.940
B>A	24.0	0.520	0.830	4.80e-2	-	-

For the CMC data, b(1) became a rather complex function of many rate constants. However, the derivations of $C_R(t_{SS})$ and $C_R(t_0)$ using $C_R(t_1)$ can be completed first, because it turns out not depend significantly on the value of b(1) for the CMC family.

With the fits for $C_R(t_1)$ in Eq. (10), the function for $C_R(t_0)$ was easily derived. The plot of $C_R(t_0)$ vs $C(t_1)$ for the Medial Family was well fitted by the same simple Excel equation for both A>B simulations and B>A simulations, with a small difference in the fitted coefficients.

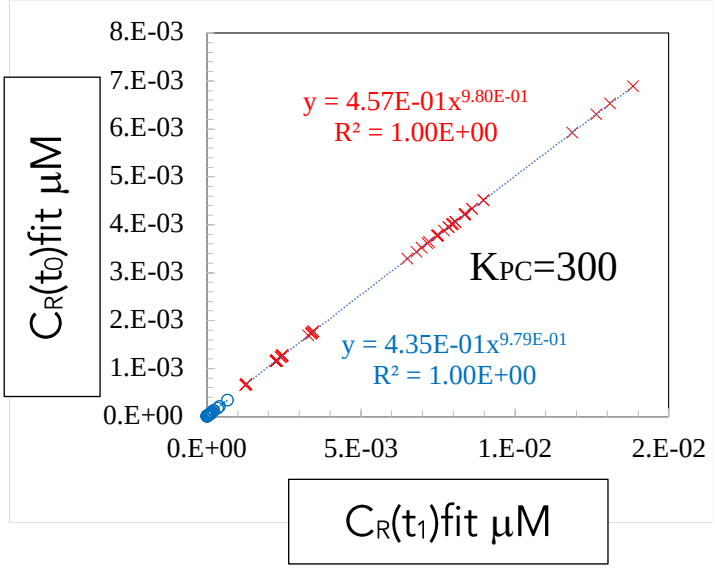

Fig. 3. Plot of $C_R(t_0)$fit vs $C_R(t_1)$fit for the Medial KP_{VD} vectors was perfectly linear, which was fitted by a power plot to facilitate the manipulation of the functions. O showed the A>B simulations and X showed the B>A simulations. The plots for the Primal family and all of the CMC families had exactly the same fitting coefficients in the Excel power function.

Therefore, the equation for the value of $C_R(t_0)$fit can be written as:

$C_R(t_0)fit=z(1)*C_R(t_1)fit^{z(2)}$ (11)

	z(1)	z(2)
A>B	0.435	0.979
B>A	0.457	0.980

The equation for the value of $C_R(t_{SS})$ was derived after discovering that the ratio of $C_R(t_{SS})/C_R(t_0)$ was fitted very simply by U_B for all simulations, including CMC, as shown in Fig.4:

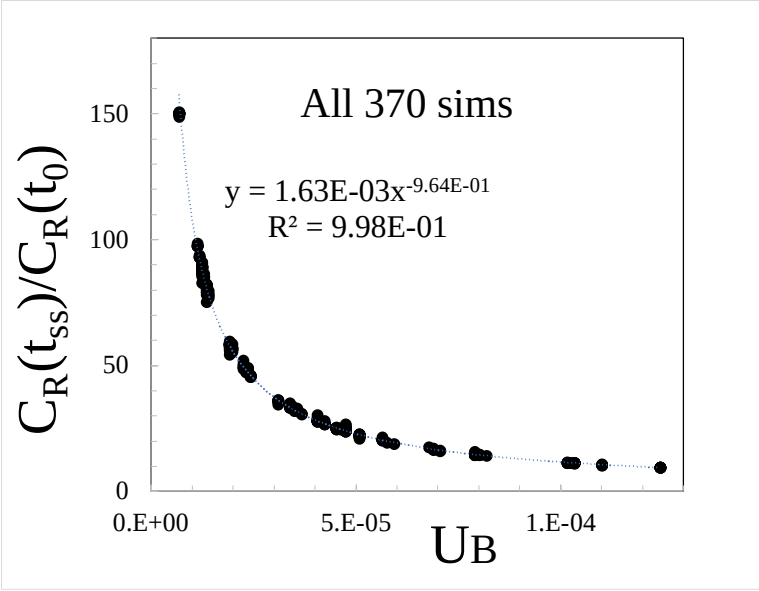

Fig. 4. Plot of $C_R(t_{SS})/C_R(t_0)$ vs U_B for all 370 KP_{VD} vectors was fitted by the Excel power function nearly perfectly.

Thus, $C_R(t_{SS})fit=1.6e\text{-}3*C_R(t_0)fit/U_B^{0.96}$ = $1.6e\text{-}3*z(1)*[C_R(t_1)fit^{z(2)}]/[U_B^{0.96}]$ (12)

The final Essential Kinetic Function to be fitted was f_H, which fits the correlations between the different avenues of transport, so its equation is likely to involve several kinetic variables. It is essentially K_{PC} & transport direction independent. f_H was not in the KP_{VD} vector because it must be fitted to the KP_{VD} simulated concentrations.

Plot of f_H vs. U_B for the 40 sims in the Primal Family

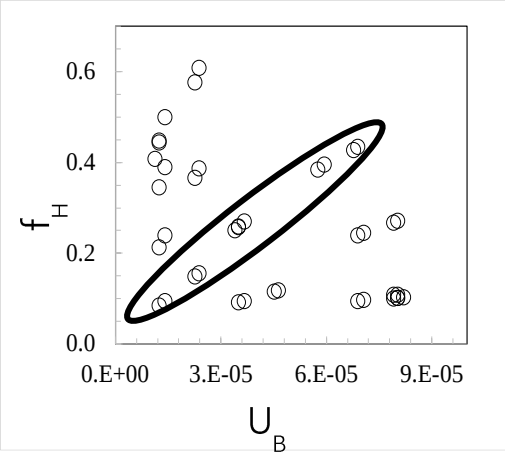

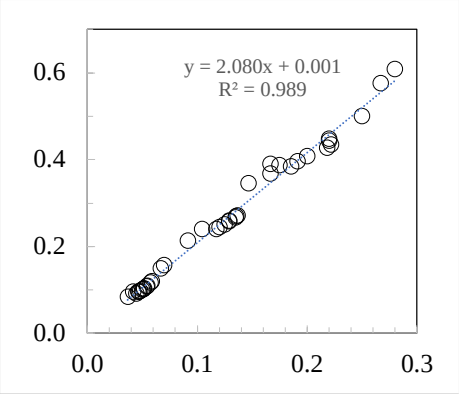

$[(P_{BC}+2.5*k_B)/(P_{AC}+P_{BC})]/(H_0+1)$

Fig. 5A. The oval highlights a possible correlated "linear" subset of 12 sims that might elucidate the equation(s) that can fit these data.

Fig. 5B. This equation shows that f_H depends on H_0, passive permeabilities and the basolateral uptake transporter.

Best fit of f_H for all 3 Families required only a small revision

f(1)=0.10 and f(2)=1.90

$f_H fit=[f(1)+f(2)*U_B/(P_{AC}+P_{BC})]/(H_0+1)$. (13)

40 PRM fits: <Rerr> = 1% <ABS(Rerr)> = 5%
126 MDL fits: <Rerr> = 1% <ABS(Rerr)> = 2%
204 CMC fits: <Rerr> = 1% <ABS(Rerr)> = 3%

Finally, the CMC family required an additional amelioration step for fitting $C_R(t_1)$ that was required for best fitting A>B transport, but not B>A transport. This was done by transforming b(1) into a function defined by the CMC KP_{VD} values:
b(1)=3.41e5+ b1cmc. (14)

This allowed the CMC equations to be accurate, while remaining aligned with Medial and Primal equations. The criteria required to assign a value to b1cmc for a new drug was based solely on the values of the rate constants. This amelioration table for the CMC KP_{VD} vectors is used in our drug fitting Excel spreadsheet for analyzing the predicted concentrations from SMAKM's fitting of experimental data, which freely is available.

Table for Amelioration of $b(1)=3.41e5+b1_{CMC}$ in the $C_R(t_1)$ function for A>B transport

U_H Subset	$<U_H$	$U_H<$	K_{PC}	k_A&k_B ranges	(H_0+1) range	m	b	$b1_{CMC}$
A1	0	4.8e-6				2.1e3	5.6e4	$m*(H_0+1) - b$
A2	4.8e-6	7.4e-6	$K_{PC}<200$			2.2e3	4.8e4	$m*(H_0+1) - b$
"			$K_{PC}>200$		≧6	5.1e9	1.1e5	$m*U_B - b$
"			"		>2.7	5.7e9	8.8e4	$m*U_B - b$
"			"		<2.7	4.2e10	5.2e4	$m*U_B - b$
B	7.4e-6	9.1e-6	$K_{PC}<200$			2.3e3	3.7e4	$m*(H_0+1) - b$
			$K_{PC}>500$			1.1e3	6.2e4	$m*(H_0+1) - b$
			200-500	k_A or $k_B>9$	<4	1.5e3	4.2e5	$m*(H_0+1) - b$
			200-500	k_A&$k_B<9$		1.16	1.6e5	$b/[(H_0+1)^m]$

U_H Subset	$<U_H$	$U_H<$	K_{PC}	k_A&k_B ranges	(H_0+1) range	m	b	$b1_{CMC}$
C	9.1e-6	1.1e-5		$abs(k_A-k_B)>3$				1.25e5
				$abs(k_A-k_B)\leqq 3$				-2e4
D	1.3e-5	1.5e-5		$min(k_A,k_B)>5$		38	8.3e4	$b - m*K_{PC}$
E	3.9e-5	4.0e-5						-1.5e4
F	4.5e-5	9.3e-5			<3			1.5e5
					>3			0

An example with a KP_{VD} vector with U_H=5.64e-6, U_B=1.2e-5, K_{PC}=300, k_A=3, k_B=1 and H_0=6

It will be in the A2 category, with m=5.7e9 and b=8.8e4. So,
b1cmc=m*U_B-b=5.1e9*1.2e-5-1.1e5 = -4.9e4.

Therefore, the Closed Form Solution for this KPVD would be best fit
with b(1)=3.41e5-4.9e4=2.9e5

After the Amelioration table was built using the CMC family KP_{VD} values, both the Medial and Primal family KP_{VD} simulation values were refitted using it. All Primal Family KP_{VD} had $b1_{CMC}$=0. The Medial Family had 19 KP_{VD} vectors refitted, but the b1cmc values were small and did not significantly change the original $C_R(t_1)$ value. There was no obvious single equation that could replace this table, so it is part of our Excel spreadsheet that fits all the functions described here for any KP_{VD} vector, including those fitted by SMAKM to our experimental data.

Random spot checks for over 70 of the Virtual Drugs showed that the value of H_0 defined by the elementary rate constants of each Virtual Drug yielded Closed Form Solution fits within experimental error.

The Closed Form Solution with all of the fitted functions of the Essential Kinetic Functions

$$C_R(t)fit = \boldsymbol{C_R(t_{SS})fit}\left[1-\left(1-\frac{\boldsymbol{C_R(t_0)fit}}{\boldsymbol{C_R(t_{SS})fit}}\right)exp\{-(H_0+1)*k_{pp}*\boldsymbol{f_Hfit}*(t-t_0)\}\right] \quad (15)$$

Accuracy of $C_R(t)fit$ Solution over all 370 simulations

A>B 40 PRM fits: <Rerr(t)> = -3% <ABS(Rerr(t))> = 4%
127 MDL fits: <Rerr(t)> = 0% <ABS(Rerr(t))> = 4%
204 CMC fits: <Rerr(t)> = 1% <ABS(Rerr(t))> = 6%

B>A 40 PRM fits: <Rerr(t)> = -2% <ABS(Rerr(t))> = 3%
127 MDL fits: <Rerr(t)> = -2% <ABS(Rerr(t))> = 4%
204 CMC fits: <Rerr(t)> = 3% < ABS(Rerr(t))> = 4%

The closed form solution is not biased toward under- or over-estimates and is sufficiently accurate to be used with experimental data to fit uptake transporter kinetics.

Conflict of Interest:

None

Acknowledgements:

None.

Funding Statement:

None.

References:

1. Zamek-Gliszczynski MJ, Lee CA, Poirier A, Bentz J, Chu X, Ellens H, Ishikawa T, Jamei M, Kalvass JC, Nagar S, Pang KS, Korzekwa K, Swaan PW, Taub ME, Zhao P, Galetin A; International Transporter Consortium. ITC recommendations for transporter kinetic parameter estimation and translational modeling of transport-mediated PK and DDIs in humans. Clin Pharmacol Ther. 2013 Jul;94(1):64-79. doi: 10.1038/clpt.2013.45. Epub 2013 Feb 25. PMID: 23588311; PMCID: PMC3898877.

2. Nagar S, Argikar UA, Tweedie DJ. Enzyme kinetics in drug metabolism: fundamentals and applications. Methods Mol Biol. 2014; 1113:1-6. doi: 10.1007/978-1-62703-758-7_1. PMID: 24523105.

3. Chu X, Prasad B, Neuhoff S, Yoshida K, Leeder JS, Mukherjee D, Taskar K, Varma MVS, Zhang X, Yang X, Galetin A. Clinical Implications of Altered Drug Transporter Abundance/Function and PBPK Modeling in Specific Populations: An ITC Perspective. Clin Pharmacol Ther. 2022 Sep;112(3):501-526. doi: 10.1002/cpt.2643. Epub 2022 Jun 21. PMID: 35561140.

4. Yamazaki S, Evers R, De Zwart L. Physiologically-based pharmacokinetic modeling to evaluate in vitro-to-in vivo extrapolation for intestinal P-glycoprotein inhibition. CPT Pharmacometrics Syst Pharmacol. 2022 Jan;11(1):55-67. doi: 10.1002/psp4.12733. Epub 2021 Nov 6. Erratum in: CPT Pharmacometrics Syst Pharmacol. 2022 Oct;11(10):1394. doi: 10.1002/psp4.12860. PMID: 34668334; PMCID: PMC8752109.

5. Galetin A, Brouwer KLR, Tweedie D, Yoshida K, Sjöstedt N, Aleksunes L, Chu X, Evers R, Hafey MJ, Lai Y, Matsson P, Riselli A, Shen H, Sparreboom A, Varma MVS, Yang J, Yang X, Yee SW, Zamek-Gliszczynski MJ, Zhang L, Giacomini KM. Membrane transporters in drug development and as determinants of precision medicine. Nat Rev Drug Discov. 2024 Apr;23(4):255-280. doi: 10.1038/s41573-023-00877-1. Epub 2024 Jan 24. PMID: 38267543.

6. Schnell S, Mendoza C (1997) Closed form solution for time-dependent enzyme kinetics. J Theor Biol 187, 207–212.

7. Acharya, P., O'Connor, M. P., Polli, J. W., Ayrton, A., Ellens, H., Bentz, J. (2008). Kinetic identification of membrane transporters that assist P-glycoprotein-mediated transport of digoxin and loperamide through a confluent monolayer of MDCKII-hMDR1 cells. *Drug Metab Dispos, 36*(2), 452-460. doi: 10.1124/dmd.107.017301

8. Agnani D, Acharya P, Martinez E, Tran TT, Abraham F, Tobin F, Ellens H, Bentz J. Fitting the elementary rate constants of the P-gp transporter network in the hMDR1-MDCK confluent cell monolayer using a particle swarm algorithm. PLoS One. 2011;6(10):e25086. doi: 10.1371/journal.pone.0025086. Epub 2011 Oct 18. PMID: 22028772; PMCID: PMC3196501.

9. Lumen AA, Acharya P, Polli JW, Ayrton A, Ellens H, Bentz J. If the K_I is defined by the free energy of binding to P-glycoprotein, which kinetic parameters define the IC50 for the Madin-Darby canine kidney II cell line overexpressing human multidrug resistance 1 confluent cell monolayer? Drug Metab Dispos. 2010 Feb;38(2):260-9. doi: 10.1124/dmd.109.029843. Epub 2009 Nov 4. PMID: 19889884.

10. Lumen AA, Li L, Li J, Ahmed Z, Meng Z, Owen A, Ellens H, Hidalgo IJ, Bentz J. Transport inhibition of digoxin using several common P-gp expressing cell lines is not necessarily reporting only on inhibitor binding to P-gp. PLoS One. 2013 Aug 16;8(8):e69394. doi: 10.1371/journal.pone.0069394. PMID: 23976943; PMCID: PMC3745465.

11. Tran, T. T., Mittal, A., Aldinger, T., Polli, J. W., Ayrton, A., Ellens, H., Bentz, J. (2005). The elementary mass action rate constants of P-gp transport for a confluent monolayer of MDCKII-hMDR1 cells. *Biophys J, 88*(1), 715-738. doi: 10.1529/biophysj.104.045633

12. Tran, T. T., Mittal, A., Gales, T., Maleeff, B., Aldinger, T., Polli, J. W., Ayrton, A., Bentz, J. (2004). Exact kinetic analysis of passive transport

across a polarized confluent MDCK cell monolayer modeled as a single barrier. *J Pharm Sci, 93*(8), 2108-2123. doi:10.1002/jps.20105

13. Butor C, Davoust J. Apical to basolateral surface area ratio and polarity of MDCK cells grown on different supports. Exp Cell Res. 1992 Nov; 203(1):115-27. doi: 10.1016/0014-4827(92)90 046-b. PMID: 1426034.

14. Whalen K, Reitzel AM, Hamdoun A. Actin polymerization controls the activation of multidrug efflux at fertilization by translocation and fine-scale positioning of ABCB1 on microvilli. Mol Biol Cell. 2012 Sep;23(18):3663-72. doi: 10.1091/mbc.E12-06-0438. Epub 2012 Aug 1. PMID: 22855533; PMCID: PMC3442413.

15. Meng Z, Ellens H, Bentz J. Extrapolation of Elementary Rate Constants of P-glycoprotein-Mediated Transport from MDCKII-hMDR1-NKI to Caco-2 Cells. Drug Metab Dispos. 2017 Feb;45 (2):190-197. doi: 10.1124/dmd.116.072140. Epub 2016 Nov 16. PMID: 27856526.

16. Meng Z, Le Marchand S, Agnani D, Szapacs M, Ellens H, Bentz J. Microvilli Morphology Can Affect Efflux Active P-Glycoprotein in Confluent MDCKII - hMDR1-NKI and Caco-2 Cell Monolayers. Drug Metab Dispos. 2017 Feb;45(2):145-151. doi: 10.1124/dmd.116.072157. Epub 2016 Nov 16. PMID: 27856525.

17. Ellens H, Meng Z, Le Marchand SJ, Bentz J. Mechanistic kinetic modeling generates system-independent P-glycoprotein mediated transport elementary rate constants for inhibition and, in combination with 3D SIM microscopy, elucidates the importance of microvilli morphology on P-glycoprotein mediated efflux activity. Expert Opin Drug Metab Toxicol. 2018 Jun;14(6):571-584. doi: 10.1080/17425255.2018.1480720. Epub 2018 Jun 7. PMID: 29788828.

18. Chaudhry A, Chung G, Lynn A, Yalvigi A, Brown C, Ellens H, O'Connor M, Lee C, Bentz J. Derivation of a System-Independent K_i for P-glycoprotein Mediated Digoxin Transport from System-Dependent IC_{50} Data. Drug Metab Dispos. 2018 Mar;46(3):279-290. doi: 10.1124/dmd.117.075606. Epub 2018 Jan 9. PMID: 29317410.

19. Bentz J, O'Connor MP, Bednarczyk D, Coleman J, Lee C, Palm J, Pak YA, Perloff ES, Reyner E, Balimane P, Brännström M, Chu X, Funk C, Guo A, Hanna I, Herédi-Szabó K, Hillgren K, Li L, Hollnack-Pusch E, Jamei M, Lin X, Mason AK, Neuhoff S, Patel A, Podila L, Plise E, Rajaraman G, Salphati L, Sands E, Taub ME, Taur JS, Weitz D, Wortelboer HM, Xia CQ, Xiao G, Yabut J, Yamagata T, Zhang L, Ellens H. Variability in P-glycoprotein inhibitory potency (IC_{50}) using various in vitro experimental systems: implications for universal digoxin drug-drug interaction risk assessment decision criteria. Drug Metab Dispos. 2013 Jul;41(7):1347-66. doi: 10.1124/dmd.112.050500. Epub 2013 Apr 25. PMID: 23620485; PMCID: PMC3684820.

20. Ellens H, Deng S, Coleman J, Bentz J, Taub ME, Ragueneau-Majlessi I, Chung SP, Herédi-Szabó K, Neuhoff S, Palm J, Balimane P, Zhang L, Jamei M, Hanna I, O'Connor M, Bednarczyk D, Forsgard M, Chu X, Funk C, Guo A, Hillgren KM, Li L, Pak AY, Perloff ES, Rajaraman G, Salphati L, Taur JS, Weitz D, Wortelboer HM, Xia CQ, Xiao G, Yamagata T, Lee CA. Application of receiver operating characteristic analysis to refine the prediction of potential digoxin drug interactions. Drug Metab Dispos. 2013 Jul;41(7):1367-74. doi: 10.1124/dmd .112.050542. Epub 2013 Apr 25. PMID: 23620486; PMCID: PMC3684818.

21. O'Connor M, Lee C, Ellens H, Bentz J. A novel application of t-statistics to objectively assess the quality of IC50 fits for P-glycoprotein and other transporters. Pharmacol Res Perspect. 2015 Feb;3(1):e00078. doi: 10.1002/prp2.78. Epub 2014 Dec 2. PMID: 25692007; PMCID: PMC4317220.